Progress In Electromagnetics Research C, Vol. 133, 195–208, 2023

Miniaturized Pentagon-Shaped Planar Monopole Antenna for Ultra-Wideband Applications

Sapna Arora[1, 2, *], Sharad Sharma[1], Rohit Anand[3], and Garima Shrivastva[4]

Abstract—A pentagon-shaped ultra-wideband (UWB) antenna with a high selective notch at the wireless local area network (WLAN) band is presented. An inverted L-shaped stub is incorporated with a pentagon-shaped metallic patch fabricated on an FR4 substrate. Also, a partial ground plane with a slot has been used to achieve UWB operation. Two structures are embedded into a patch to realize a rectangular notch. An electromagnetic band gap (EBG) structure is placed on the opposite side of the patch, and a rectangular complementary split ring resonator (RCSRR) is embedded in the patch. With the coupling of two structures, their notch bands are adjusted to achieve a rectangular notch. The bandwidth, upper and lower frequencies of the notch can be adjusted by varying dimensions of RCSRR and EBG. The measured and simulated results show $S_{11} \leq -10$ dB for 3.1 GHz–12.5 GHz with a notch at the WLAN band from 5 GHz to 5.91 GHz. Also, the proposed design has a stable radiation pattern and gain with a peak value of 3.5 dB at 9.5 GHz and -6 dB at 5.1 GHz. The miniaturized size of the proposed design (21.5 mm $\times$ 27.5 mm $\times$ 1.6 mm) with ultra-wide bandwidth makes it suitable for wireless applications.

1. INTRODUCTION

For short-range communications, the next generation is ultra-wideband (UWB) communication. UWB has inherent improvements in terms of enhanced immunity to interference because of discrimination in direct and orthogonal reflected waves. Due to low-duty cycle impulses, power requirements are extremely low [1]. The use of impulse pulses spreads information over wide bandwidth which leads to high security. These UWB features increase its use for high-speed indoor communications and make it suitable for battery-dependent appliances.

According to the broad definition, a UWB system operates on a bandwidth at least equal to 500 MHz or bandwidth that is 20% of the center frequency being used [2]. Federal Communication Commission released the spectrum of 3.1 GHz–10.6 GHz for commercial UWB use in 2002 [3]. But many license bands exist in the UWB range and cause interference such as worldwide interoperability for microwave access (WiMAX) from 3.3 GHz to 3.6 GHz, Wireless local area network (WLAN) from 5.15 GHz to 5.825 GHz, and X-band satellite communication from 7.25 GHz to 7.75 GHz. The most suitable technique to avoid interference from these bands is the use of a UWB antenna with notch characteristics at the initial point of the UWB system. Because of the planar structure's light weight and ease of integrity with electronic components, microstrip patch antenna has attracted antenna designers [4, 5]. Various approaches have been applied to achieve patch antennae with notch characteristics. Some of the examples are the use of electromagnetic band gap structures [6, 7], slots with different shapes [8, 9], split rings resonators [10, 11], Integrated Passive Device (IPD) Technology [12], micro-electro-mechanical

Received 11 March 2023, Accepted 30 May 2023, Scheduled 6 June 2023

* Corresponding author: Sapna Arora (sapnaarora1@gmail.com).

[1] MM(DU), Mullana, Ambala, Haryana, India. [2] Panipat Institute of Engineering & Technology, Haryana, India. [3] G. B. Pant DSEU Okhla-1 Campus (formerly GBPEC), New Delhi, India. [4] NSUT East Campus, New Delhi, India.

system (MEMS) capacitors [13], nonuniform periodical slotted ground [14], coupling with parasitic elements [15], and defective ground structures [16, 17].

It is worth noting that the techniques mentioned above have the drawback of the regular notch with imperfect selectivity depicted in Fig. 1, which is not the optimum choice for blocking wide interference bands, i.e., WLAN band. Many design techniques have been used to implement the WLAN band discussed in [18–22]. In [18], a rectangular patch with a U-shape slot creates a notch at 4.9–6.1 WLAN band with peak rejection at 5.5 GHz having voltage standing wave ratio (VSWR) equal to 4. An elliptic single complementary split ring resonator in patch [19] has been used to implement a notch from 5.12 GHz–6.07 GHz with peak VSWR at 5.73 GHz. A coplanar waveguide (CPW)-fed circular antenna is suggested in [20] with split rings to eliminate the notch at the WLAN band having a range 5.393–5.822 GHz. A circular patch antenna connected with $\lambda/4$ slot line-resonator can block the WLAN band of 5.01 GHz–6.19 GHz [21]. In [22] a horizontal slot is introduced in the patch to notch the WLAN band from 5.1 GHz–5.82 GHz.

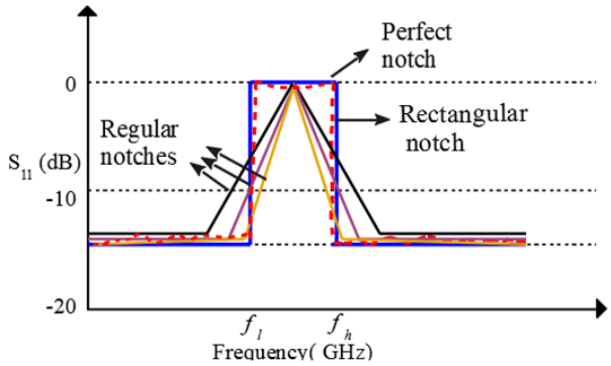

Figure 1. Regular, rectangular and perfect notch.

The designs discussed above have two drawbacks. Firstly, the notch achieved at the WLAN band with the above techniques has poor selectivity. Secondly, the regular notch offers the highest rejection to central frequency and less rejection to other frequencies present in the notch band. The reason behind the problems is band rejection in UWB antennas implemented by a single notch-creating element for one band. So, it becomes difficult to achieve high-frequency selectivity and equal suppression for all frequencies in the notch band. Fig. 1 demonstrates the difference between regular notches, rectangular notch, and perfect notch. A rectangular notch can eliminate both the problems discussed above. In current years, some antennas with sharp notch characteristics are being investigated. In [23], a rectangular antenna having size 47 mm × 38 mm can suppress the WiMAX band with a C-shape slot in the patch, and U-shape slot resonators present on both sides of the feed line provide sharp notches for lower WLAN (5.15–5.35 GHz) and upper WLAN (5.725 GHz–5.825 GHz). Thus, it provides sharp electivity, but spiculated notch does not solve the second problem. In [24], an urn shape radiator makes use of one T-shape stub and C-shaped slots to produce high band rejection for WiMAX, WLAN, and X-band but with poor selectivity. A differential stepped-slot UWB antenna blocks 5.1 GHz–6 GHz with quarter wavelength slits incise in-ground and 7.83 GHz–8.47 GHz by a half wavelength stub with wide notch characteristics [25] but having complex geometry.

In [26, 27], the authors suggest that to achieve wideband rejection with high selectivity, two notch-creating elements are required for a single band. In [26], an elliptical patch antenna is proposed with two EBGs introduced on the CPW feeding line to create a wide notch with the benefit of controlled notch bandwidth. Here, the resonant frequencies of EBGs are tuned in such a way that notch bands created by two EBGs overlap each other to produce rectangular notch characteristics. In [27], a slit in patch and strip in the ground plane are used in an asymmetric coplanar strip (ACS)-fed antenna. The coupling of the strip and slit creates a rectangular notch band with controllable bandwidth. However, the structures suggested in both works of literature exhibit large and complex geometry. Hence, the UWB antenna with a simplified and compact configuration is required to create a rectangular notch band with sharp selectivity having bandwidth-controlled features.

This work presents a pentagon-shaped compact UWB planar antenna loaded with a stub to achieve wide impedance bandwidth. The coupling of EBG and rectangular complementary split ring resonator (RCSRR) provides a rectangular notch for WLAN, and by tuning the parameters of both structures, the bandwidth is controlled. The proposed design aims to increase the antenna bandwidth with a controlled rectangular notched WLAN band and minimize the dimensions to make it fit for wireless applications.

2. ANTENNA CONFIGURATION

2.1. Antenna Geometry

The proposed design is shown in Fig. 2. The design contains a pentagonal shape patch fed with a 50-ohm microstrip line. To increase the bandwidth of radiating patch, it is connected with an inverted L-shape stub and partial ground plane with a slot on another side of the substrate. The design is printed on a low-cost FR4 substrate having a size of 21.5 mm × 27.5 mm × 1.6 mm. One EBG structure is made up of a small rectangular metal patch, and a shorting pin is connected to the radiator to obtain a notch at the WLAN band. EBG structure acts as a filter by absorbing the current at a specific frequency range thereby blocking radiation from the patch. Also, an RCSRR is incorporated with the design to

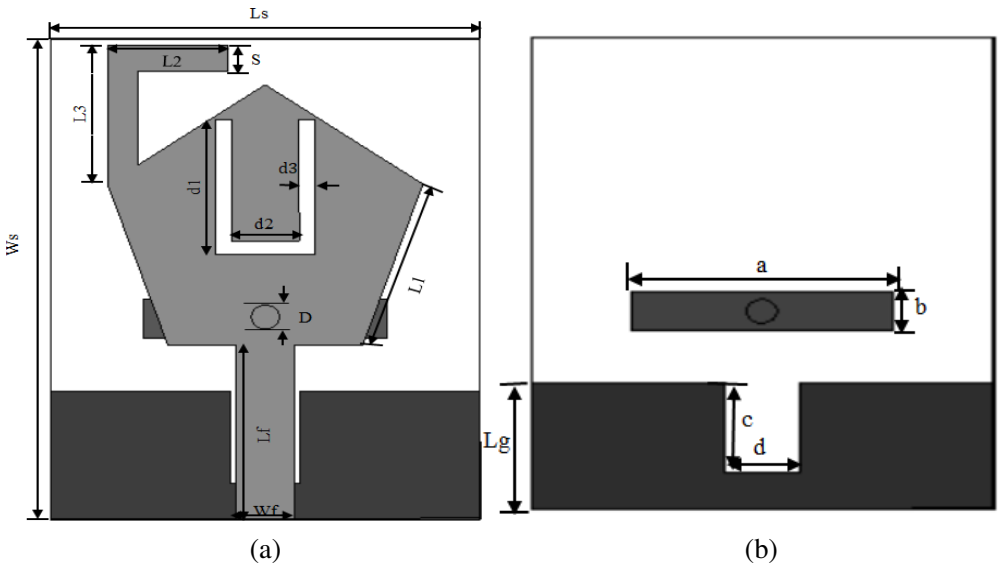

Figure 2. Proposed design. (a) Front view. (b) Back view.

Table 1. Proposed antenna parameters with their values.

Parameter	Value (mm)	Parameter	Value (mm)
Ls	21.5	Wf	2.9
Ws	27.5	a	12.2
Lg	7.4	b	2.2
$L1$	8.3	c	5.3
$L2$	6	d	3.5
$L3$	8	$d1$	7
s	1.5	$d2$	5
$L4$	6.5	$d3$	0.8
Lf	10.32	D	1.4

obtain desired wide-notch characteristics. The slot resonator and EBG can be easily embedded in the patch and its opposite side respectively without any increase in size and complexity. This antenna is simulated in Ansys High-Frequency Structure Simulator (HFSS), and parameters are optimized through parametric analysis. The dimensions of the proposed design are mentioned in Table 1.

2.2. Design Steps of the Proposed Antenna

To get the proposed design, a step-by-step procedure is shown in Fig. 3. First, the techniques to achieve a basic antenna with UWB characteristics are shown in steps (a), (b), and (c). Design 1 presents a planar pentagon monopole antenna (PPMA) designed by equating the area of the pentagon to the area of the monopole antenna with a cylindrical shape [28].

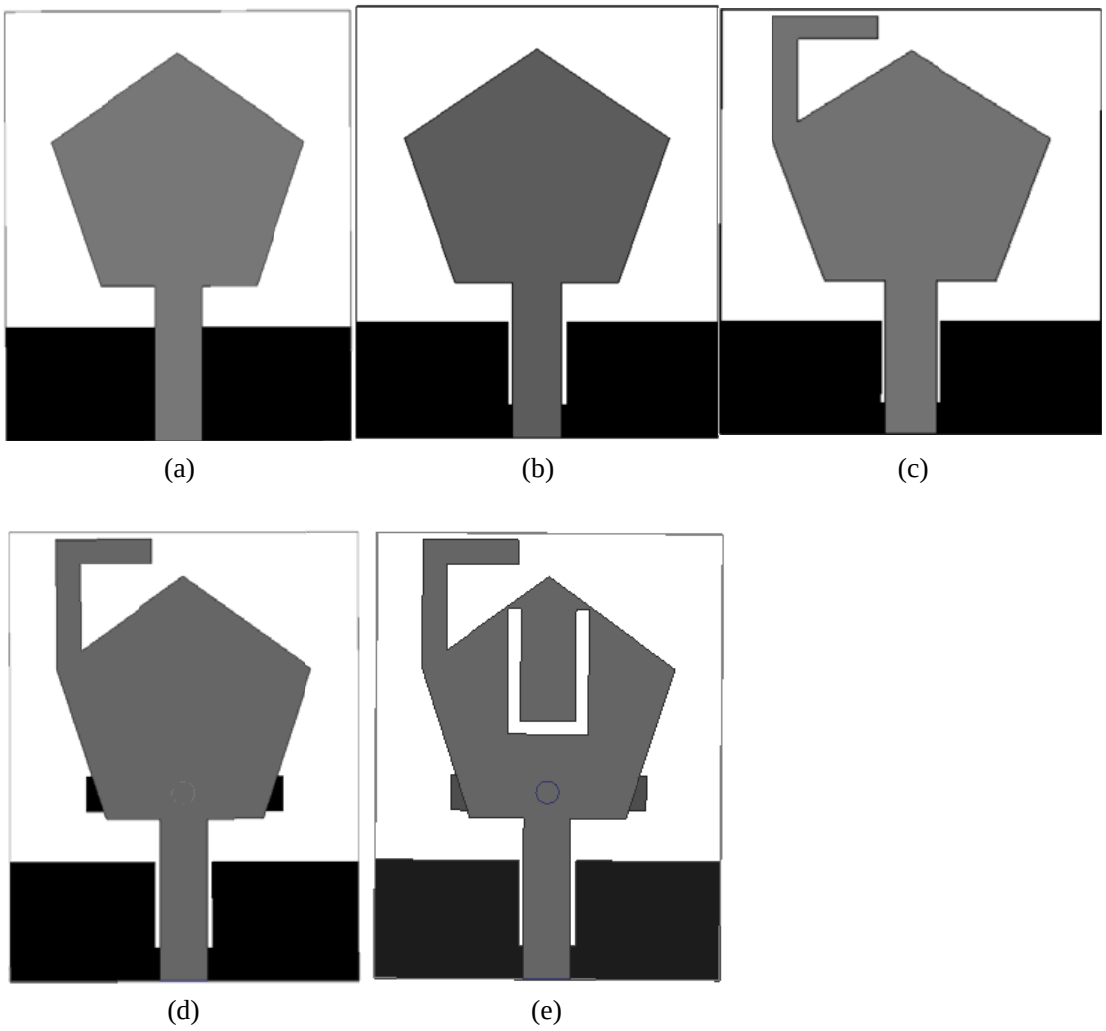

Figure 3. Design steps. (a) Design 1. (b) Design 2. (c) Design 3. (d) Design 4. (e) Proposed design.

If $L1$ is the side length and H the height of PPMA, then

$$H = L1\frac{\sqrt{5+2\sqrt{5}}}{2} \tag{1}$$

The height H of PPMA is taken equal to the height of an equivalent monopole antenna with a cylindrical shape.

The frequency at the lower band edge is given below

$$f_L = \frac{c}{\lambda} = \frac{7.2}{[(L + r + p)\, k]}\,\text{GHz}$$

Here L is the height, and r is the radius of the cylindrical-shape monopole antenna in cm. Here p is a gap between the upper edge of the partial ground plane and the lower edge of the patch. For a PPMA with dimensions $L1 = 0.976\,\text{cm}$ and $p = 0.25\,\text{cm}$, $c_r = 4.4$, the calculated value of f_L is 3.25 GHz, against the simulated value of 3.54 GHz which is within 10% of the calculated value. The impedance bandwidth of design 1 is from 3.54 GHz to 8.47 GHz for a magnitude of $S_{11} \leq -10\,\text{dB}$ as shown in Fig. 4.

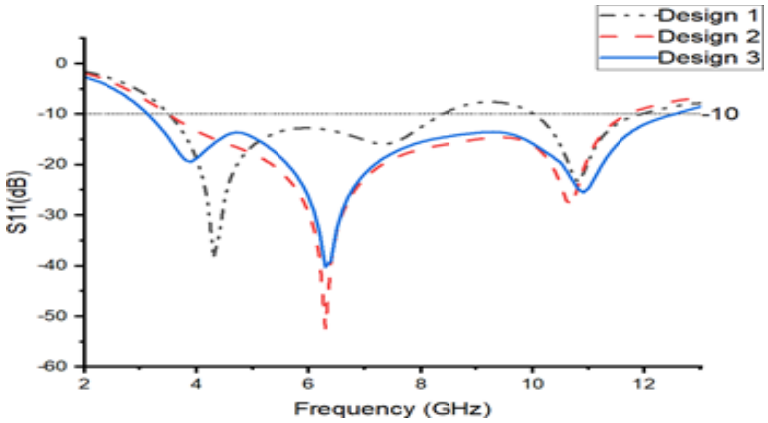

Figure 4. The simulated S_{11} for different steps shown in Figs. 3(a), (b) & (c).

To further increase the bandwidth, in design 2 a slot is etched in the partial ground plane under the feed line. This slot introduces capacitance which cancels the patch inductance, and input impedance becomes nearly resistive at higher frequencies. Now bandwidth has been achieved from 3.6 GHz to 11.78 GHz as shown in Fig. 4. To decrease the lower edge frequency, the inverted stub is incorporated on the upper edge of the patch [26] in design 3. Fig. 4 shows that impedance bandwidth varies from 3.1 to 12.5 GHz for $S_{11} \leq -10\,\text{dB}$ which satisfies the UWB criteria proposed by Federal Communications Commission (FCC). Also, design 3 provides a Z_{11} curve with $\text{Re}(Z_{11})$ as $50\,\Omega$ and $\text{Im}(Z_{11})$ close to $0\,\Omega$ for the complete UWB which verifies impedance matching for 3.1 GHz to 12.5 GHz as shown in Fig. 6.

2.3. Design of UWB Antenna with Wide Rectangular Notch Band

The rectangular notch is obtained by the coupling of two structures, RCSRR engraved in the patch and EBG loaded on the opposite side of the substrate. By parametric analysis, their dimensions are adjusted in such a way that RCSRR creates a rejection band from 5 GHz–5.31 GHz, and the EBG structure has notching characteristics ranging 5.28 GHz–5.91 GHz. Thus, the two structures resonating ranges overlap each other creating a desired wide notch.

2.3.1. Electromagnetic Bandgap Structure

EBG structure acts as a bandstop filter due to its bandgap property. Its equivalent circuit is a parallel LC resonator, and the resonant frequency is given by:

$$f_{\text{ebg}} = \frac{1}{2\pi\sqrt{\text{LC}}}$$

Here L is the inductance and C the capacitance which are calculated using equations [29].

Here

$$L = \mu_0 h$$

and

$$C = \frac{w\varepsilon_0(\varepsilon_r + 1)}{2} \cosh^{-1}\left\{\frac{2w+g}{g}\right\}$$

where h is the height of the substrate, w the width of EBG, g the gap between two cells of EBG, μ_0 the permeability, ε_0 the permittivity of free space, and ε_r the dielectric constant of the substrate. This resonant frequency varies with changes in the dimensions of the EBG structure. In Fig. 3(d), an EBG structure having length a and width b is loaded at the opposite side of the substrate and linked to a pentagon patch with a metallic via having diameter D.

Here length a and width b are optimized to obtain a regular notch having a range from 5.28 GHz to 5.91 GHz as shown in Fig. 5. The imaginary impedance of design 4 falls to $-79\,\Omega$, and the real impedance rises to $113\,\Omega$ causing a mismatch in impedances, resulting in $S_{11} > -10$ dB obtained for 5.28 GHz–5.91 GHz as depicted in Fig. 6(a). But this classic notch does not block the WLAN band completely. So there is a need for another band-stop filter discussed in the next section.

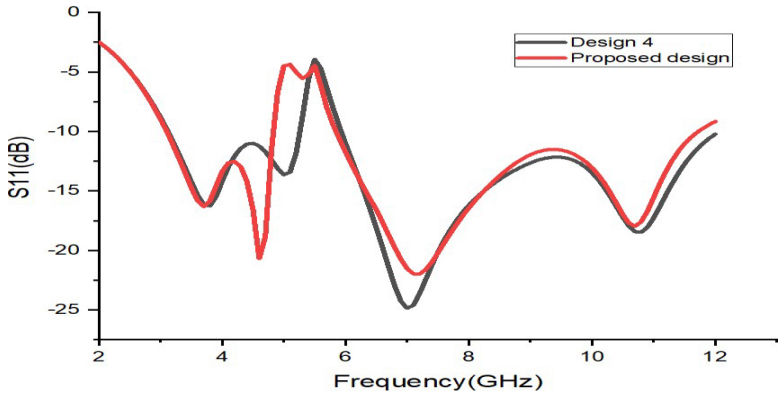

Figure 5. Reflection coefficient characteristics of design 4 and proposed design.

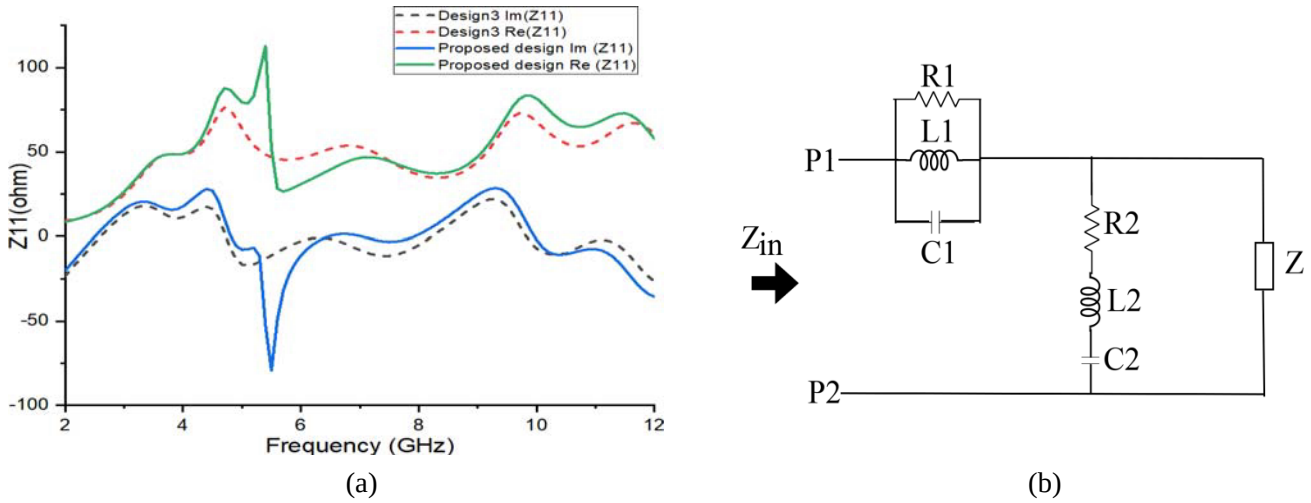

Figure 6. (a) Impedance characteristic of design 3 and proposed design. (b) Lumped equivalent circuit of the proposed design.

2.3.2. Rectangular Complementary Split Ring Resonator

RCSRR exhibits the property of a band-stop filter. Its horizontal and vertical lengths decide the resonant frequency. To get an initial idea about RCSRR dimensions, design equations have been used.

The notch band frequency f_{RCSRR} [30] is given by

$$f_{\text{RCSRR}} = \frac{C}{2(d1 + 2d2)\sqrt{\varepsilon_{eff}}} \tag{2}$$

where $L1$ is the vertical length, $L2$ the horizontal length, and c the speed of light. For 5 GHz–5.3 GHz, center frequency is 5.15 GHz, thereby Equation (4) gives $L1 + 2L2 = 17.7$ mm. After parametric simulations, the optimal value of $L1 + 2L2 = 16.5$ mm and $d3 = .8$ mm is obtained.

2.3.3. Lumped Equivalent Circuit of the Proposed Antenna

The equivalent circuit can be derived by the impedance curve as discussed in [31, 32]. The impedance curve containing both the real and imaginary curves of the proposed antenna is presented in Fig. 6(a). At the center frequency 5.59 GHz, the value of the real part of the impedance is 124 ohm, and the imaginary part has a negative slope, which acts like a parallel RLC circuit. At 5.91 GHz the value of $\text{Re}(Z_{11})$ is 25 ohm, and $\text{Im}(Z_{11})$ has a positive slope, which acts like a series RLC network. Hence the equivalent circuit for the WLAN notch is given by cascading series connection of parallel RLC circuit with series RLC circuit. The RLC circuit of the proposed antenna is shown in Fig. 6(b). Here block Z represents the input impedance of the UWB antenna, which is the series connection of several parallel RLC circuits.

3. PARAMETRIC ANALYSIS OF PROPOSED DESIGN AND SURFACE CURRENT DISTRIBUTIONS

To investigate the effect of different parameters of RCSRR and EBG, parametric analysis has been performed. In this analysis, one parameter is swept while others are constant. The effect of changing the length $d1$ of RCSRR is shown in Fig. 7. From the S_{11} curve, it is clear that notch width decreases from 5–5.825 GHz to 5.2–5.68 GHz as the value of $d1$ decreases from 7 mm to 6.5 mm. This is because slot length is inversely proportional to antenna bandwidth, thus decrease in slot length tends to decrease notch width and hence increase impedance bandwidth $S_{11} \leq -10$ dB. Thus bandwidth can be controlled by changing the length of RCSRR.

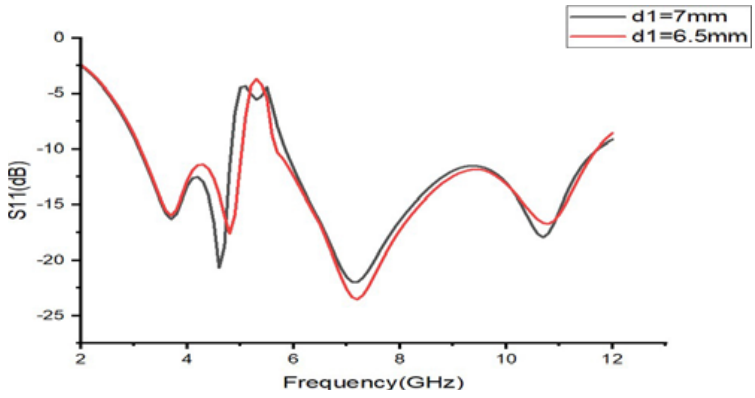

Figure 7. Effect of RCSRR length on the bandwidth of proposed design.

Variation in lower frequency with different EBG widths (2.1 mm, 2.2 mm, 2.3 mm) has been investigated, and an optimum value of 2.3 mm is selected from the analysis. Fig. 8 shows that the lower notch frequency shifts to the left side as the width of EBG, i.e., b, is increased and has a negligible effect on the upper frequency, hence the width of EBG controls the lower frequency. The variation in upper frequency can be seen in Fig. 9. The gap between the slot and EBG is responsible for controlling upper frequency. As the gap increases from 1.2 mm to 2 mm, upper frequency also increases showing little effect on lower and passband frequencies. Thus optimum value for the gap chosen is 2 mm in the proposed antenna.

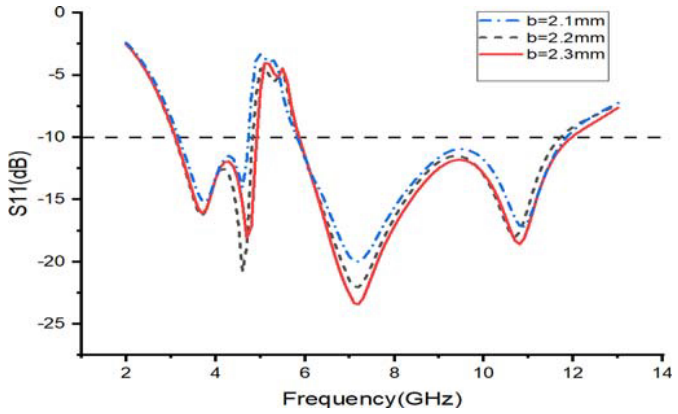

Figure 8. Effect on EBG width on a lower frequency of proposed design.

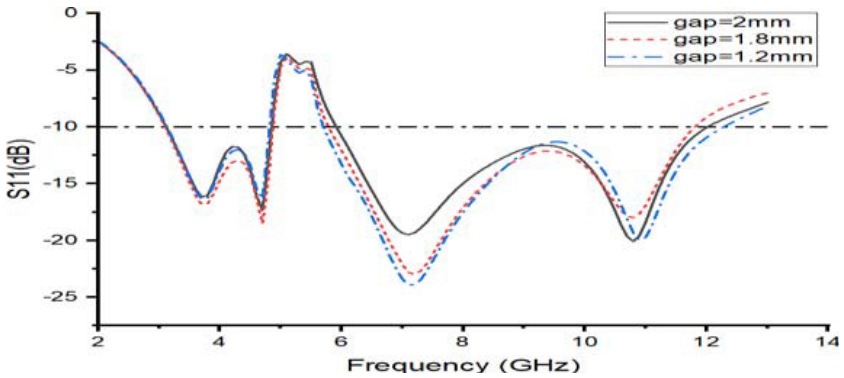

Figure 9. Effect of the varying gap between EBG structure and RCSRR.

To further investigate the proposed design, surface current distributions (J_{surf}) are shown in Fig. 10. In Figs. 10(a) and (b), current distributions at multiple frequencies are displayed.

It is clear from the current distributions shown in Figs. 10(a) and 10(b) that EBG and CSRR structures have almost no effect on passband frequencies. However in Fig. 10(c), more current is present near the slot at 5.15 GHz depicting the resonance of RCSRR, and power is not radiated from the patch thus creating a notch at this frequency. Also, at 5.59 GHz in Fig. 10(d), a large current is surrounded by an EBG structure which depicts its resonance and another notch from 5.28 GHz to 5.91 GHz. Fig. 10(e) at 5.44 GHz shows that current surrounds both structures and thus overlaps two resonances, thereby creating a wide notch for the WLAN band.

4. MEASURED RESULTS AND ANALYSIS

The proposed design was fabricated to validate the simulated results. The front and back views of the fabricated design are shown in Fig. 11(a) and Fig. 11(b), respectively. The reflection coefficient S_{11} for fabricated design is measured with ANRITSU (Model #MS 2038C) vector network analyzer (VNA). The measured and simulated reflection coefficient graphs are shown in Fig. 12.

Measured results show that the proposed design rejects 5.1 GHz–5.89 GHz frequency band while preserving UWB performance from 3.1 GHz–12.5 GHz. There is good matching in the two graphs except at higher frequencies. The difference in the results is mainly due to the tolerances in fabrication.

Figure 12(b) shows the simulated and measured gains of the proposed design. The highest gain obtained at 9.5 GHz has a value of 3.5 dB and falls abruptly to 6 dB at the notch band. Thus, the proposed design can reject the WLAN band and pass UWB frequencies ranging from 3.1 GHz to 12.5 GHz successfully.

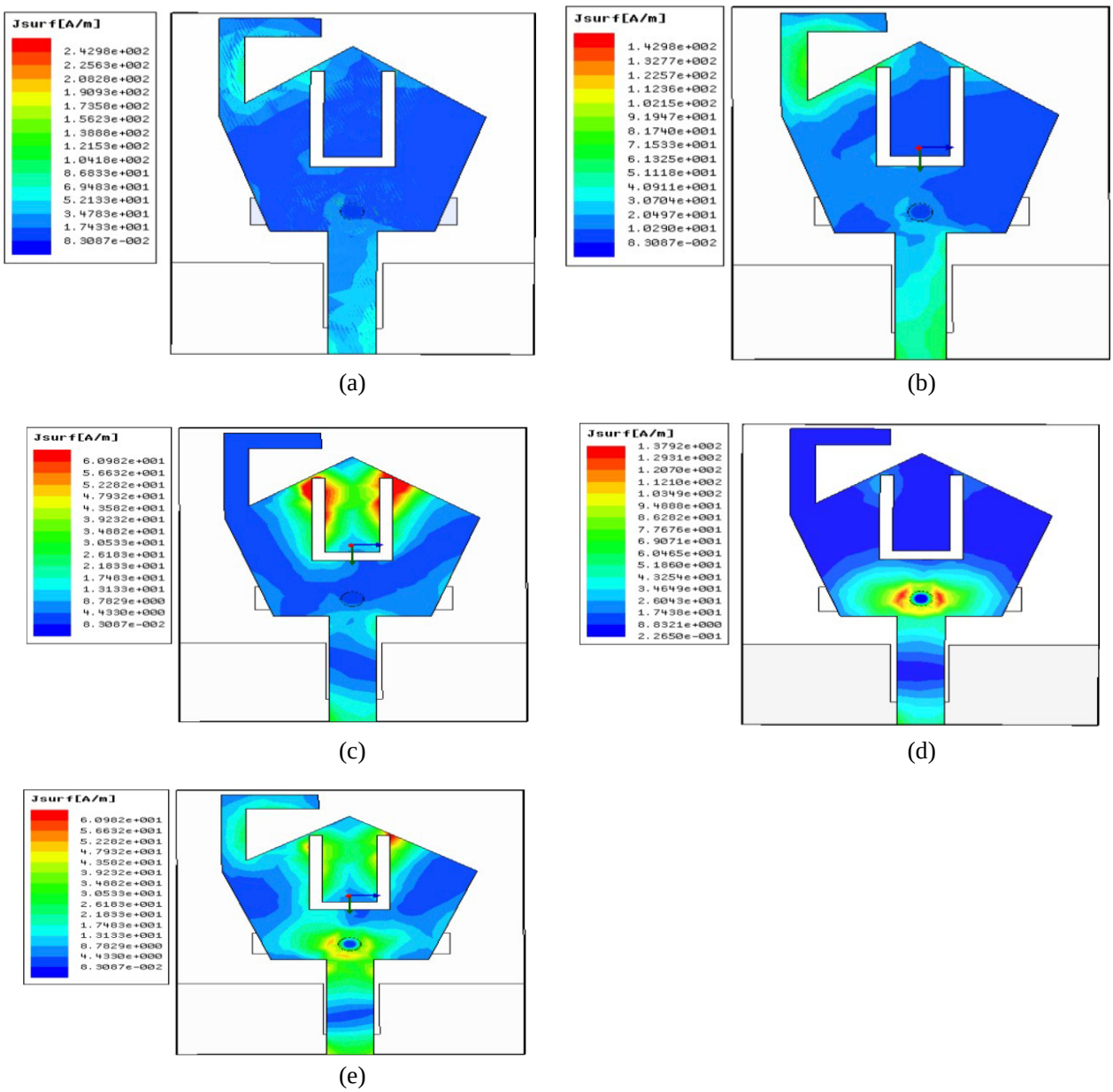

Figure 10. Surface current distributions at (a) 3.9 GHz, (b) 6.3 GHz, (c) 5.15 GHz, (d) 5.59 GHz, (e) 5.44 GHz.

The proposed antenna placed in a microwave-protected anechoic chamber for radiation pattern measurement is shown in Fig. 13(a). In Fig. 13(b), ANRITSU MS 2038C VNA Master in Spectrum Analyzer Mode is shown to measure the peak power of the proposed antenna (used as a receiving antenna) in Spectrum Analyzer. At a particular frequency, the reading of peak power is measured (from the Spectrum Analyzer) which can be used to calculate the gain of the proposed antenna. From this gain, the radiation pattern can be plotted at each of the desired frequencies.

The radiation patterns at H-plane and E-plane at 3.6 GHz, 4.6 GHz, and 7.2 GHz are shown in Fig. 14. To measure the radiation patterns in the anechoic chamber, a Horn antenna is used as the transmitting antenna, and the proposed fabricated design acts as the receiving antenna.

The received power is calculated by rotating the receiving antenna at different angles. Then by using the FRIIS equation, the gain of receiving antenna is measured and drawn. The H-plane radiation patterns are nearly omnidirectional and symmetrical. E-plane radiation patterns are bidirectional as

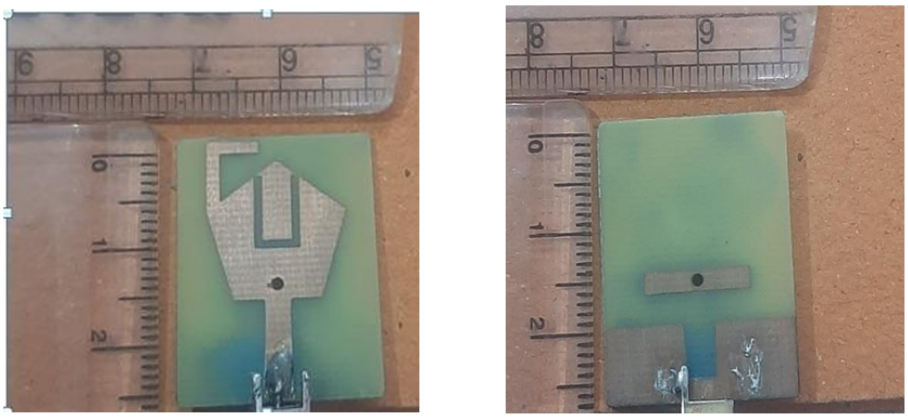

(a) (b)

Figure 11. Fabricated antenna design. (a) Front view. (b) Back view.

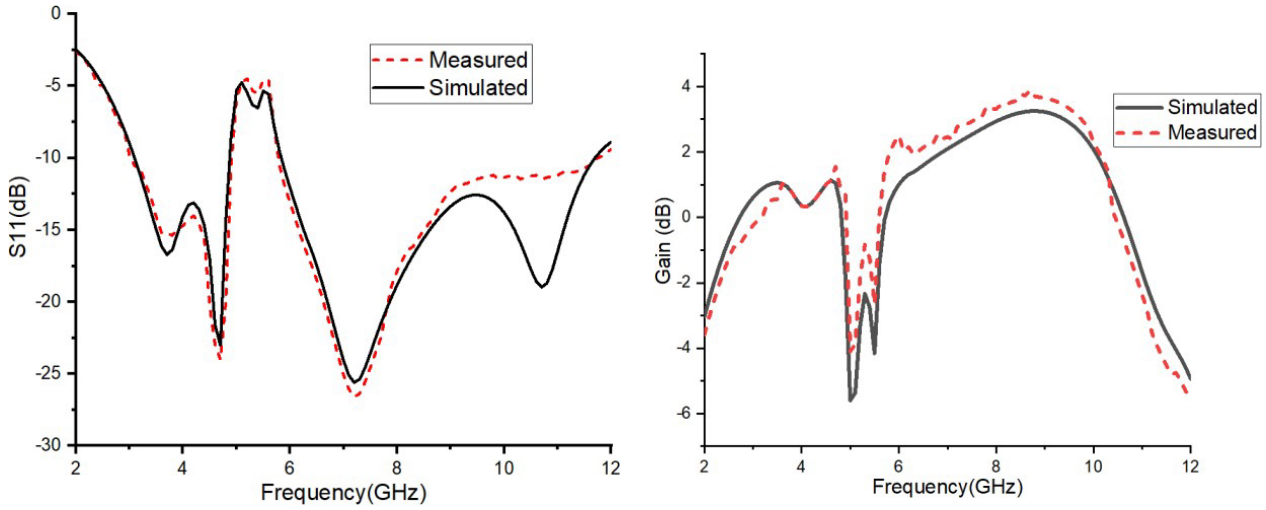

(a) (b)

Figure 12. Simulated and measured results for (a) S_{11}, (b) gain.

(a) (b)

Figure 13. (a) Antenna under test in anechoic chamber, (b) power measurement in spectrum analyzer.

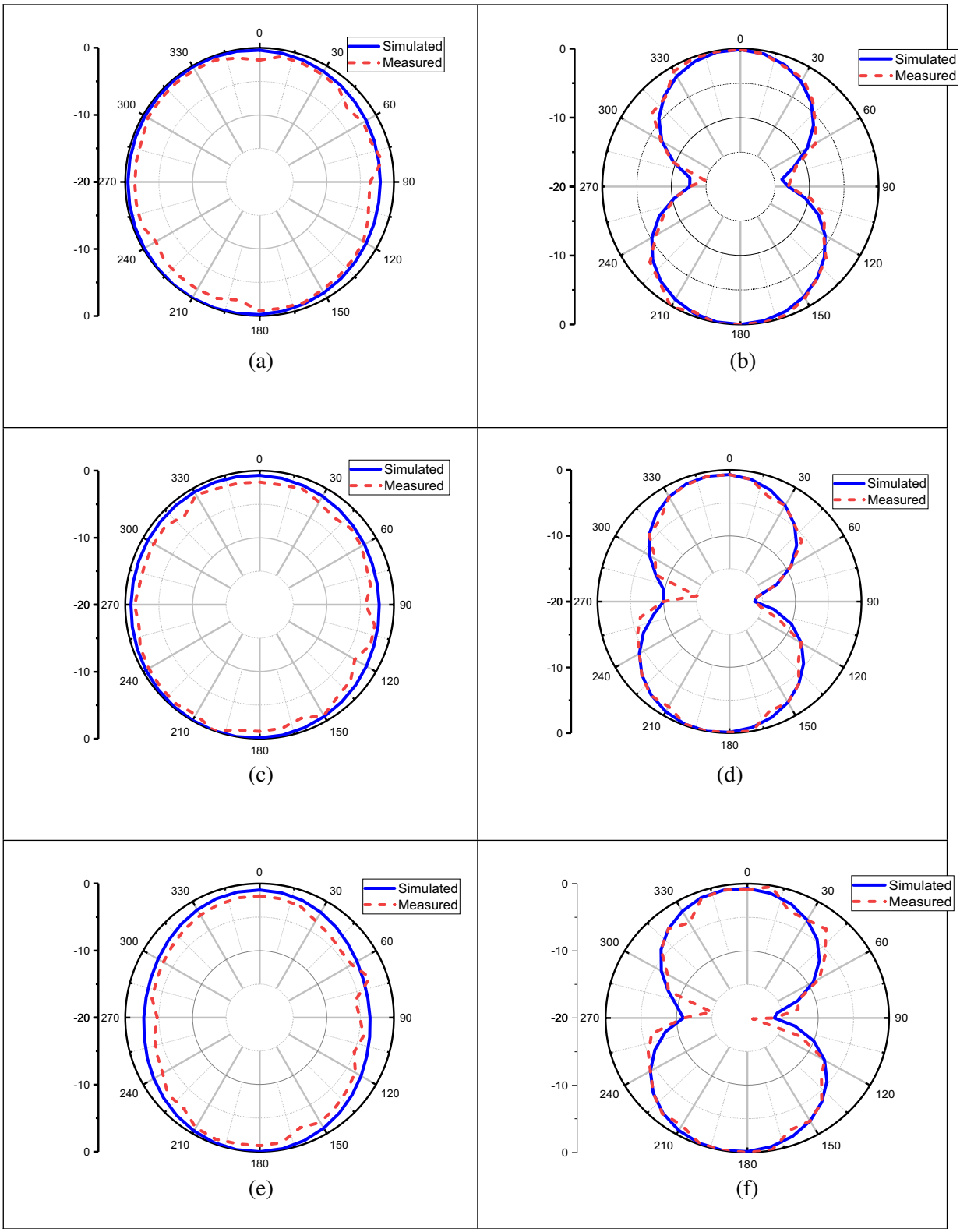

Figure 14. Radiation patterns in H-plane, and an E-plane at 3.6 GHz, 4.6 GHz, and 7.2 GHz. (a) H-plane at 3.6 GHz. (b) E-plane at 3.6 GHz. (c) H-plane at 4.6 GHz. (d) E-plane at 4.6 GHz. (e) H-plane at 7.2 GHz. (f) E-plane at 7.2 GHz.

Table 2. Comparison of the proposed design with existing WLAN band-notched antenna in the literature.

Referred Antennas	Size of Antenna (mm^3)	Notched Bandwidth (GHz)	Controlled Notch Bandwidth	Rectangular notch
[33]	$50 \times 48 \times 1$	4.92–6.16	NO	YES
[34]	$35 \times 35 \times 0.8$	15.725–5.825	NO	NO
[35]	$13 \times 22 \times 0.8$	4.9–6	NO	NO
[36]	$20 \times 20 \times 0.8$	5.03–5.94	YES	NO
Proposed design	$21.5 \times 27.5 \times 1.6$	5–5.91	YES	YES

shown in Fig. 14. The measured results are well matched with simulated ones.

Before concluding this work the antenna is compared with already existing WLAN band notched antennas [33–36] based on size, type, and bandwidth of notch as shown in Table 2. Most of the designs are large and do not offer controlled bandwidth features except [36]. The antennas proposed in [33, 34] are large and reject WLAN bandwidth, which also includes useful frequencies. In [35, 36], although antennas are small in size, and both structures create regular notches at the WLAN bandwidth with poor selectivity. In brief, the proposed design with simple geometry and small size successfully created a rectangular WLAN notch with good selectivity.

5. CONCLUSION

UWB antenna with a rectangular notch and controlled bandwidth fabricated on an FR4 substrate having size 21.5 mm × 27.5 mm × 1.6 mm with a simple geometry is presented. The rectangular WLAN notch is achieved by the coupling of complementary RCSRR and EBG structures. Also, notched bandwidth can be controlled by varying dimensions and distance between notch-creating structures. For this purpose, parametric analysis has been discussed in detail. Due to its small size and ultra-wide bandwidth, this antenna is a good candidate for hand-held devices used in wireless applications.

REFERENCES

1. Fontana, R. J., "Recent system applications of short-pulse ultra-wideband (UWB) technology," *IEEE Transactions on Microwave Theory and Techniques*, Vol. 52, No. 9, 2087–2104, 2004.
2. Fowler, C., J. Entzminger, and J. Corum, "Assessment of ultra-wideband (UWB) technology," *IEEE Aerospace and Electronic Systems Magazine*, Vol. 5, No. 11, 45–49, 1990.
3. Federal Communications Commission, "In the matter of revision of Part 15 of the commission's rules regarding ultra-wideband transmission systems," *First Report and Order*, ET Docket 98-153, 2002.
4. Anand, R., S. Arora, and N. Sindhwani, "A miniaturized UWB antenna for high-speed applications," *2022 International Conference on Computing, Communication and Power Technology (IC3P)*, 264–267, IEEE, January 2022.
5. Anand, R. and P. Chawla, "A novel dual-wideband inscribed hexagonal fractal slotted microstrip antenna for C- and X-band applications," *International Journal of RF and Microwave Computer-Aided Engineering*, Vol. 30, No. 9, e22277, 2020.
6. Jaglan, N., B. K. Kanaujia, S. D. Gupta, and S. Srivastava, "Design and development of efficient EBG structures based band-notched UWB circular monopole antenna," *Wireless Personal Communications*, Vol. 96, No. 4, 5757–5783, 2017.
7. Yazdi, M. and N. Komjani, "Design of a band-notched UWB monopole antenna by means of an EBG structure," *IEEE Antennas and Wireless Propagation Letters*, Vol. 10, 170–173, 2011.

8. Chibber, A., R. Anand, and S. Arora, "A staircase microstrip patch antenna for UWB applications," *2021 9th International Conference on Reliability, Infocom Technologies and Optimization (Trends and Future Directions) (ICRITO)*, 1–5, IEEE, September 2021.
9. Arora, S., S. Sharma, and R. Anand, "A survey on UWB textile antenna for Wireless Body Area Network (WBAN) applications," *Artificial Intelligence on Medical Data: Proceedings of International Symposium, ISCMM 2021*, 173–183, Springer Nature Singapore, Singapore, July 2022.
10. Hamad, E. K. and N. Mahmoud, "Compact tri-band notched characteristics UWB antenna for WiMAX, WLAN, and X-band applications," *Advanced Electromagnetics*, Vol. 6, No. 2, 53–58, 2017.
11. Chen, X., F. Xu, and X. Tan, "Design of a compact UWB antenna with triple notched bands using nonuniform width slots," *Journal of Sensors*, 2017.
12. Luo, C. M., J. S. Hong, and H. Xiong, "A tri-band-notched UWB antenna with low mutual coupling between the band-notched structures," *Radioengineering*, Vol. 22, No. 4, 1233–1238, 2013.
13. Sousa Neto, M. P., H. C. Fernandes, and C. G. Moura, "Design of a ultrawideband monopole antenna using split ring resonator for notching frequencies," *Microwave and Optical Technology Letters*, Vol. 56, No. 6, 1471–1473, 2014.
14. Kim, D.-O., N.-I Jo, H.-A. Jang, and C.-Y. Kim, "Design of the ultrawideband antenna with a quadruple-band rejection characteristics using a combination of the complementary split ringresonators," *Progress In Electromagnetics Research*, Vol. 112, 93–107, 2011.
15. Azim, R., M. T. Islam, and A. T. Mobashsher, "Design of a dual band-notch UWB slot antenna by means of simple parasitic slits," *IEEE Antennas and Wireless Propagation Letters*, Vol. 12, 1412–1415, 2013.
16. Sanyal, R., P. P. Sarkar, and S. Sarkar, "Octagonal nut shaped monopole UWB antenna with sextuple band notched characteristics," *AEU-International Journal of Electronics and Communications*, Vol. 110, 152833, 2019.
17. Baudha, S. and M. V. Yadav, "A novel design of a planar antenna with modified patch and defective ground plane for ultra-wideband applications," *Microwave and Optical Technology Letters*, Vol. 61, No. 5, 1320–1327, 2019.
18. Hussain, N., M. Jeong, J. Park, S. Rhee, P. Kim, and N. Kim, "A compact size 2.9–23.5 GHz microstrip patch antenna with WLAN band-rejection," *Microwave and Optical Technology Letters*, Vol. 61, No. 5, 1307–1313, 2019.
19. Sarkar, D., K. V. Srivastava, and K. Saurav, "A compact microstrip-fed triple band-notched UWB monopole antenna," *IEEE Antennas and Wireless Propagation Letters*, Vol. 13, 396–399, 2014.
20. Premalatha, B., M. V. S. Prasad, and M. B. R. Murthy, "Compact penta band notched antenna using concentric rings with splitter bricks for ultra wide band applications," *Journal of Communications Technology and Electronics*, Vol. 63, No. 12, 1379–1385, 2018.
21. Lee, C. H., J. H. Wu, C. I. G. Hsu, H. L. Chan, and H. H. Chen, "Balanced band-notched UWB filtering circular patch antenna with common-mode suppression," *IEEE Antennas and Wireless Propagation Letters*, Vol. 16, 2812–2815, 2017.
22. Yadav, A., R. P. Yadav, and A. Alphones, "CPW fed triple band notched UWB antenna: Slot width tuning," *Wireless Personal Communications*, Vol. 111, No. 4, 2231–2245, 2017.
23. Habash, M. F., A. S. Tantawy, H. A. Atallah, and A. B. Abdel-Rahman, "Compact size triple notched-bands UWB antenna with sharp band-rejection characteristics at WiMAX and WLAN bands," *Advanced Electromagnetics*, Vol. 7, No. 3, 99–103, 2018.
24. Sharma, M., Y. K. Awasthi, H. Singh, R. Kumar, and S. Kumari, "Compact printed high rejection triple band-notch UWB antenna with multiple wireless applications," *Engineering Science and Technology, An International Journal*, Vol. 19, No. 3, 1626–1634, 2016.
25. Althuwayb, A. A., M. Alibakhshikenari, B. S. Virdee, P. Shukla, and E. Limiti, "Realizing UWB antenna array with dual and wide rejection bands using metamaterial and electromagnetic band gaps techniques," *Micromachines*, Vol. 12, No. 3, 269, 2021.

26. Peng, L., B. J. Wen, X. F. Li, X. Jiang, and S. M. Li, "CPW fed UWB antenna by EBGs with wide rectangular notched-band," *IEEE Access*, Vol. 4, 9545–9552, 2016.
27. Xiong, X. P., Q. Liu, Y. Zhang, and Y. L. Luo, "Novel ACS-fed monopole antenna for UWB applications with sharp selectivity notched band and additional Bluetooth band characteristics," *Journal of Electromagnetic Waves and Applications*, Vol. 28, No. 18, 2308–2317, 2014.
28. Ray, K. P., "Design aspects of printed monopole antennas for ultra-wide band applications," *International Journal of Antennas and Propagation*, 2008.
29. Sievenpiper, D., L. Zhang, R. F. Broas, N. G. Alexopolous, and E. Yablonovitch, "High-impedance electromagnetic surfaces with a forbidden frequency band," *IEEE Transactions on Microwave Theory and Techniques*, Vol. 47, No. 11, 2059–2074, 1999.
30. Dattatreya, G., K. Kousalya, Y. Jyothirmayi, M. V. Krishna, D. Harsha, P. A. V. Sri, and K. K. Naik, "Analysis of complementary split ring resonators on rectangular patch with inset feed for X-band application," *2017 International conference of Electronics, Communication and Aerospace Technology (ICECA)*, Vol. 2, 248–250, IEEE, April 2017.
31. Nosrati, A., M. Mohammad-Taheri, and M. Nosrati, "Dual-to-quad-band evanescent-mode substrate-integrated waveguide band-pass filters," *IET Microwaves, Antennas & Propagation*, Vol. 14, No. 11, 1229–1240, 2020.
32. Nosrati, A., M. Mohammad-Taheri, and M. Nosrati, "Gap-coupled dual-band evanescent-mode substrate integrated band-pass filter waveguide," *Progress In Electromagnetics Research Letters*, Vol. 89, 53–59, 2020.
33. Peng, L., B. J. Wen, X. F. Li, X. Jiang, and S. M. Li, "CPW fed UWB antenna by EBGs with wide rectangular notched-band," *IEEE Access*, Vol. 4, 9545–9552, 2016.
34. Dalal, P. and S. K. Dhull, "Upper WLAN band notched UWB monopole antenna using compact two via slot electromagnetic band gap structure," *Progress In Electromagnetics Research C*, Vol. 100, 161–171, 2020.
35. Hussain, N., M. Jeong, J. Park, S. Rhee, P. Kim, and N. Kim, "A compact size 2.9–23.5 GHz microstrip patch antenna with WLAN band-rejection," *Microwave and Optical Technology Letters*, Vol. 61, No. 5, 1307–1313, 2019.
36. Ojaroudi, M. and N. Ojaroudi, "Ultra-wideband small rectangular slot antenna with variable band-stop function," *IEEE Transactions on Antennas and Propagation*, Vol. 62, No. 1, 490–494, 2013.